GEOPHYSICAL RESEARCH LETTERS, VOL. 24, NO. 1, PAGES 25-28, JANUARY 1, 1997

Relationship between tropical upper tropospheric moisture and eastern tropical Pacific sea surface temperature at seasonal and interannual time scales

Reginald E. Newell and Yong Zhu

Department of Earth, Atmospheric and Planetary Sciences, Massachusetts Institute of Technology, Cambridge, Massachusetts

William G. Read and Joe W. Waters

Jet Propulsion Laboratory, California Institute of Technology, Pasadena, California

Abstract. Water vapor in the tropical upper troposphere, above the altitudes ordinarily sampled by radiosonde humidity elements, is important in controlling atmospheric infrared energy loss to space, both by its dominance of infrared transmission and its role in cloud formation. Much of the water vapor arrives in the upper troposphere above about 12 km in plumes associated with cumulonimbus complexes; values at 215 and 147 hPa have recently been estimated from the Microwave Limb Sounder on the NASA Upper Atmosphere Research Satellite. In equatorial regions, time changes of upper troposphere moisture over a three year period, 1991-1994, are closely related to sea surface temperature changes in the eastern tropical Pacific, including seasonal and non-seasonal variations. Maps of the annual and semi-annual components at 215 and 147 hPa show maxima over the eastern hemisphere land masses and the maritime continent, as well as over Central and South America.

Introduction

Above about 10 km (pressure equivalent of 300 hectopascals [hPa]), water vapor measurements by conventional radiosonde techniques have not been reliable until recently. The Microwave Limb Sounder (MLS) on the NASA Upper Atmosphere Research Satellite (UARS) can observe water vapor when the radiometer used to monitor ClO in the stratosphere, which operates at about 205 GHz (wavelength of ~1.5 mm), is scanned down through the troposphere (Read et al., 1995). While the best sensitivity is at about 150 parts per million by volume (ppmv), preliminary algorithms have been constructed to yield data at 215 hPa (~12 km) and 147 hPa (~14.2 km). Although numerical values are assigned, the preliminary nature of the algorithms is recognized by using the term MLS UTH (upper tropospheric humidity). These two levels provide information above the conventional radiosonde altitudes and in regions where outflow from cumulonimbus complexes is often observed (Webster and Stephens, 1980; Wang et al., 1995; Newell et al., 1996b). UARS is at 585 km altitude in a circular 57° orbit, and with 15 orbits a day and a limb scan every 4.1° of orbit arc, it yields a total of about 1300 vertical profiles a day. The horizontal projection on the earth's surface of an individual limb scan is about 400 km x 400 km. Due to the limb viewing geometry with no capacity to scan in azimuth, there are large measurement gaps between the orbit tracks. Details of the data reduction process and the role of convective cirrus anvils in this process have been presented by Read et al. (1995); ice has a generally negligible effect at concentrations less than 0.01 gm m^{-3}, and about a 20% effect if present at 0.1 gm m^{-3}, if spread over 120 km horizontally. The latter value exists only in strong convective systems. The accuracy at 215 hPa is estimated to be about 40%; more *in situ* intercomparisons are needed to improve on this, as the data from standard radiosondes used to construct climatologies are not reliable at these high altitudes. The precision is thought to be 5 ppmv or less. Measurements commenced on 21 September 1991 and are continuing, but with severely interrupted operations between November 1994 and September 1995. Mean maps at 215 hPa for December-February 1991-1993 and June-August 1992-1993 have been published (Read et al., loc. cit.), as well as maps coincident with the NASA Pacific Exploratory Mission West, which was carried out using a DC-8 aircraft in September-October 1991 (PEM-West A) and February-March 1994 (PEM-West B) (Newell et al., 1996b). During PEM-West A, the water vapor data were compared with an on-board Lyman-α hygrometer (Newell et al., 1996a). This comparison shows a tendency for MLS UTH values to be too high for mixing ratios less than 200 ppmv. However, there were too few points in this comparison to derive a numerical correction factor that could be used here.

The main point here is that when monthly zonal mean values of MLS UTH are computed, there is, in addition to the expected seasonal changes, a substantial year-to-year variability of water vapor at 215 hPa in the equatorial regions, which is shown to be related to sea surface temperature variations in the eastern equatorial Pacific.

Procedure and Results

Monthly mean maps were drawn up for October 1991 to March 1996, with the exception of the gap noted above and other shorter gaps evident in a recent presentation of the zonal means (Elson et al., 1996). From two examples shown (Figure 1), it can be seen that the maximum MLS water vapor at 215 hPa (about 12 km) reflects the general patterns of water vapor obtained by the radiosonde network at 400 hPa (about 7.5 km), as mapped by Rasmusson, 1972. This early work

Paper number 96GL03776.
0094-8534/97/96GL-03776$05.00

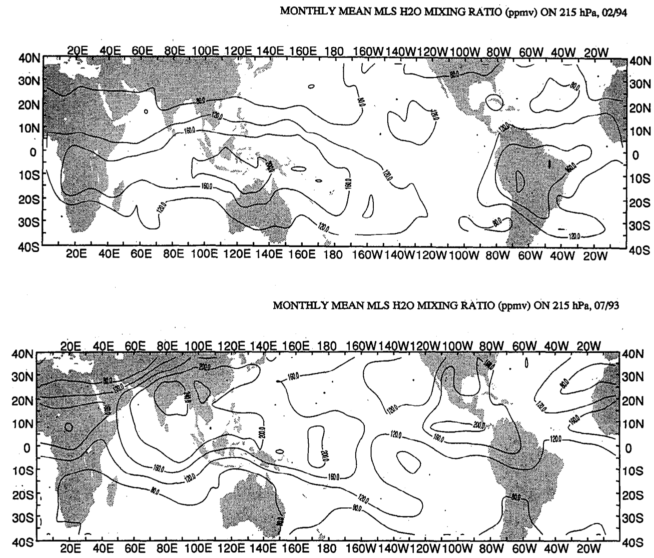

Figure 1. Maps of UARS water vapor at 215 hPa for months of February 1994 (a) and July 1993 (b). Units, ppmv.

included a number of island stations covering the ocean, but the coverage has deteriorated since then. At 215 hPa and 147 hPa there are maxima in the Intertropical Convergence Zone (ITCZ) south of the equator over the western Pacific and over Africa and South America in February, and maxima over Panama and the ocean to the west, Central Africa, and the Indian monsoon region trailing southeastwards into the South Pacific Convergence Zone in July. The overall maximum occurs in July-August and is associated with the intense moisture plume over the Indian continent. There is strong subsidence and dryness over the eastern Mediterranean not far from this plume in July, with dryness in the southeast Pacific and South Atlantic. Upwelling and subsidence regions were classified from the divergent wind component, examples of which have been given elsewhere (Newell et al., 1996b).

Zonal mean latitudinal profiles of water vapor at both pressure levels were constructed for each month by collecting all data at a given pressure into 5°-wide latitude bands. These showed systematic changes in the same month from one year to the next; time series at 5° latitude intervals between ±35° were drawn to study these changes. These time series fell into three categories: Northern Hemisphere seasonal cycles with maxima at 20°-35°N, mostly in August, as is the case for free air temperature over the ocean; Southern Hemisphere seasonal cycles with maxima at 15°-30°S, centered on mid-February; and a non-seasonal variation over the 5° latitude belt, centered on the equator. The monthly means for the region from 30°N to 30°S were subjected to harmonic analysis, and maps of the amplitudes of the annual and semi-annual components are illustrated in Figure 2. Maximum amplitudes for the annual component are generally over the land masses, particularly Asia, with extensions eastwards from the Eastern Hemisphere continents. Minimum amplitudes occur near the equator over much of the globe, as well as over the southeastern Pacific. The semi-annual component is also generally larger over land, with an extension over the Atlantic to the northeast of Brazil. Cross sections of zonal means of these two harmonic components were drawn (not shown) and accentuate the minimum in the annual component in the 0°-5°N region, and they also show a maximum in the semi-annual component at about 5°N. The cross sections were compared with those of mean zonal wind and temperature; mean zonal wind also has a substantial semi-annual amplitude between 100 and 200 hPa in the 20°N to 20°S region (Newell et al., 1974), as of course do many other parameters in the tropical free troposphere (Hu, 1995).

Water vapor non-seasonal variations in the 5° latitude strip centered on the equator for 147 and 215 hPa are closely related to non-seasonal sea surface temperature (SST) over the equatorial eastern Pacific in the region generally known as the Niño 1 and Niño 2 area, which covers the region 80°-90°W, 0°-10°S (NOAA, 1996) (Figure 3). Although the absolute values of SST and H_2O have a strong similar seasonal variation in this region, the anomalies from the three-year means for water vapor and for SST are also correlated. For the 36 months of this three-year sample, the correlation between SST, supplied by R.W. Reynolds and evaluated following the procedure described by Reynolds and Smith (1995), and water vapor zonal means in the tropical strip, is 0.75, so that SST changes

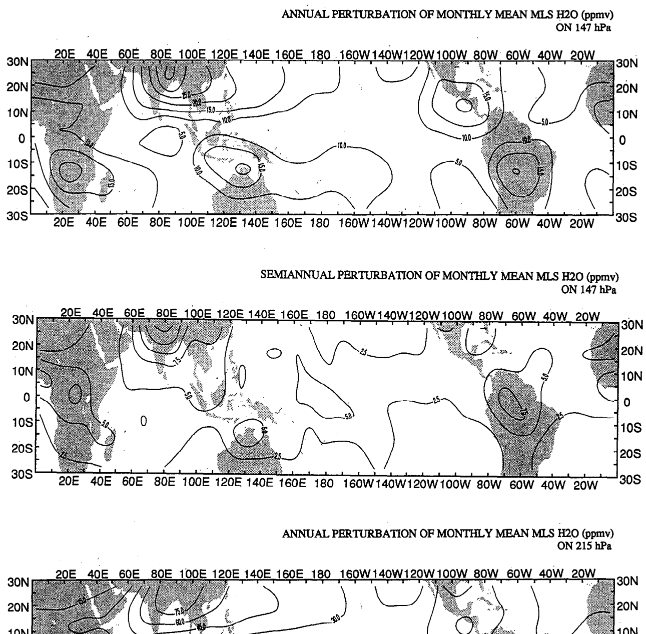

Figure 2. Maps of annual and semi-annual amplitudes from a harmonic analysis of UARS water vapor at 215 hPa and 147 hPa. Units, ppmv. (a): Annual amplitude, 147 hPa; (b): Semi-annual amplitude, 147 hPa; (c): Annual amplitude, 215 hPa; (d): Semi-annual amplitude, 215 hPa.

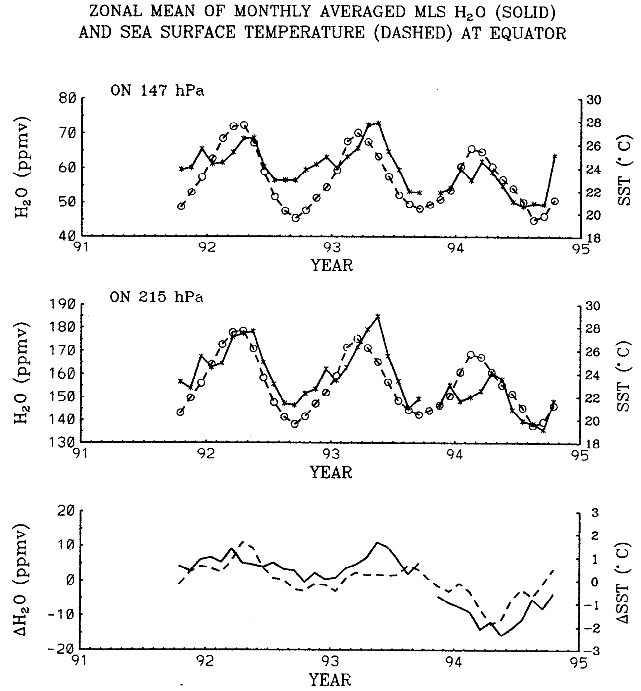

Figure 3. Time series, covering October 1991-October 1994, of zonal mean 147 hPa and 215 hPa water vapor, evaluated monthly in 5° latitude belt centered on equator and eastern equatorial monthly mean sea temperature in El Niño 1 and 2 region. Note that H_2O values for October 1993 are missing. Lower panel: H_2O at 215 hPa (solid) and SST (dashed) anomalies for same regions as used above. Units, H_2O: ppmv; SST: °C.

account for about 56% of the variance of the water vapor fluctuations, if auto-correlation between the anomalies is ignored. The water vapor differences between April 1992 and April 1994 (Figure 4) are about 20-40 ppmv, well above the 5 ppmv precision quoted earlier. While the maximum difference is in the central and eastern tropical Pacific, the higher values in 1992 are carried round the tropics in a similar fashion to the lateral spreading in February and July shown in Figure 1. It is worth noting that the maximum differences in water vapor between 1992 and 1994 occur in the April-May season. April is the month when the meridional convergence of water vapor in the lower layers near the equator is a maximum, due to the combined effects of transports by mean and eddy motions (Rasmusson, 1972). It is therefore clear that motions within the tropics are related to the observed water vapor changes.

Comparison With Previous Studies

The MLS UTH data cover a region that is quite distinctive in the tropics, as may be seen in Figure 5, which illustrates a relative humidity meridional cross-section along 147.5°E. The regions of high humidity (>90%) spread out over much of the tropics above about 10 km. This occurs even above regions where the humidity is only 20% at 8 km. Examples of individual lidar images of cirrus taken during February 1994, the period used for Figure 5 (Newell et al., 1996b), showed cirrus originating in the ITCZ near 10°S and moving as far north as Guam (14°N). The great lateral extent of cirrus has been known for some time (Webster and Stephens, 1980), and examination of the winds makes it clear that the moistening

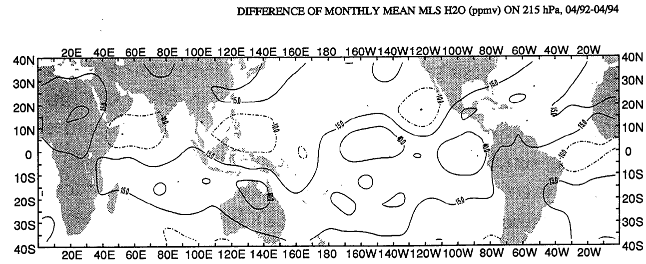

Figure 4. Map of 215 hPa water vapor difference between April 1992 and April 1994. Units, ppmv.

ability of this cirrus can be carried round the globe in the tropics. Studies confined to radiosonde altitudes (~10 km) would not necessarily reflect changes in this layer.

Prior work related non-seasonal tropical temperature changes to eastern equatorial Pacific SST (PSST) changes (Newell and Weare, 1976; Pan and Oort, 1983), and radiosonde moisture changes to PSST changes (Pan and Oort, loc. cit.; Wu, 1996). Some satellite water vapor data from the Stratospheric Aerosol and Gas Experiment (SAGE II) are available to well above 50 hPa, but have only been used to study seasonal changes, not interannual changes (Rind et al., 1991). Interannual variations of highly reflective cloud and enhanced rising motion in the tropical eastern Pacific have been found to be related to PSST by Zimmerman et al. (1988). Tropical cirrus clouds in the 11-18 km layer were examined with SAGE II and their interannual variability found to be related to PSST (Kent et al., 1995). As for Zimmerman et al. (1988), their interpretation involves changes in the Hadley-Walker tropical circulation system. Water vapor in the upper troposphere (200-500 hPa), deduced from 6.7 μm radiance where the weighting function peaks at about 300 hPa, has been related to PSST by Soden and Fu (1995), and Fu et al. (1996) have also studied the high cloud variability as mentioned above. Bates et al. (1996) have related water vapor from the high resolution infrared sounder instruments (HIRS) to PSST. Their relatively high (low) brightness temperatures indicate a relatively dry (moist) upper troposphere. Water

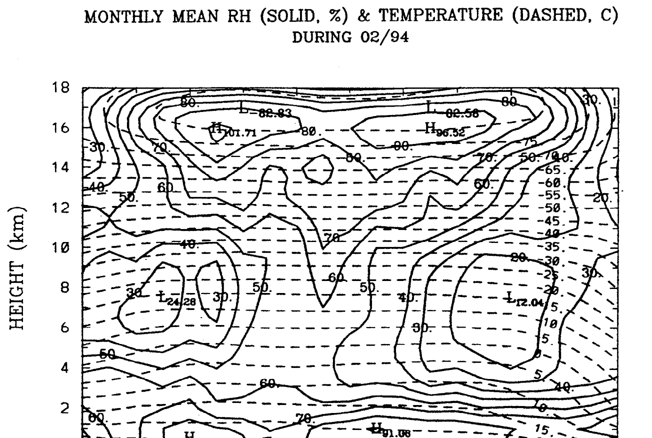

Figure 5. Cross-section along 147.5°E of relative humidity and temperature for February 1994. Units, RH: %; temperature: °C.

vapor profile variability is more important than temperature profile variability in determining brightness changes. They used the brightness temperature to trace deep convection and increased upper tropospheric moisture during ENSO events in 1982/83, 1986/87 and 1991/93. Because their instrumental weighting function peaks at about 250 hPa in moist and 350 hPa in dry conditions, they cannot always have been viewing the region above 10-12 km evident in Figure 5 that seems to be strongly tied to overall deep convection. Seasonal variations of UTH showing a positive relationship with convection have been made by Stephens et al. (1996), also using satellite radiance data at 6.7 µm.

What is reported here is that water vapor in the critical region between 200 and 100 hPa, which is dominated by outflow of ice crystals from the deep convection regions in the 15°N-15°S tropical strip and covers a region far greater than that of the active convection, varies directly with the SST changes in the eastern tropical Pacific on a non-seasonal basis. During El Niño, as Wu (1996) has shown, above-average evaporation occurs from the eastern equatorial Pacific, amounting to about 40 Wm^{-2} locally but averaging to about 1 Wm^{-2} over the 15°N-15°S tropical strip. The additional moisture convergence, latent heat liberation and convection in the central and western Pacific is thought to be responsible for injection of additional moisture into the ~200-100 hPa layer, which moisture is then spread over the tropics. Because the water vapor in this region is important in controlling atmospheric infrared energy loss to space and in controlling cirrus cloud formation outside the deep convection regions, which are related to larger scale vertical motion, factors controlling the water vapor mixing ratio are important in understanding climatic fluctuations.

Acknowledgements. We acknowledge support from NASA Grant NAG-1-1252 and the NSF Climate Dynamics Program Grant ATM-9422512, and thank the European Center for Medium-Range Weather Forecasts for their provision of grid point data used in Figure 5.

References

Bates, J. J., X. Wu, and D. L. Jackson, Interannual variability of upper-troposphere water vapor band brightness temperature, *J. Climate, 9*, 427-438, 1996.

Elson, L. S., W. G. Read, J. W. Waters, P. W. Mote, J. S. Kinnersley, and R. S. Harwood, Space-time variations in water vapor as observed by the UARS Microwave Limb Sounder, *J. Geophys. Res., 101*, 9001-9015, 1996.

Fu, R., W. T. Liu, and R. E. Dickinson, Response of tropical clouds to the interannual variation of sea surface temperature, *J. Climate, 9*, 616-634, 1996.

Hu, W., The Semi-Annual Cycle of Sea Surface and Free Air Temperatures, S.M. thesis, 57 pp., MIT, Cambridge, Mass., June 1995.

Kent, G. S., E. R. Williams, P.-H. Wang, M. P. McCormick, and K. M. Skeens, Surface temperature related variations in tropical cirrus cloud as measured by SAGE II, *J. Climate, 8*, 2577-2594, 1995.

National Oceanic and Atmospheric Administration, *Climate Diagnostics Bulletin No. 96/9*, p. 10, Washington DC, 1996.

Newell, R. E., J. W. Kidson, D. G. Vincent and G. J. Boer, *General Circulation of the Tropical Atmosphere Vol. 2*, 371 pp., MIT, Cambridge, Mass., 1974.

Newell, R. E. and B. C. Weare, Factors governing tropospheric mean temperature, *Science, 194*, 1413-1414, 1976.

Newell, R. E., Y. Zhu, E. V. Browell, S. Ismail, W. G. Read, J. W. Waters, K. K. Kelly, and S. C. Liu, Upper tropospheric water vapor and cirrus: Comparison of DC-8 observations, preliminary UARS microwave limb sounder measurements and meteorological analyses, *J. Geophys. Res., 101*, 1931-1941, 1996a.

Newell, R. E., Y. Zhu, E. V. Browell, W. G. Read and J. W. Waters, Walker circulation and tropical upper tropospheric water vapor, *J. Geophys. Res., 101*, 1961-1974, 1996b.

Pan, Y. H. and A. H. Oort, Global climate variations connected with sea surface temperature anomalies in the Eastern Equatorial Pacific Ocean for the 1958-73 period, *Mon. Wea. Rev., 111*, 1244-1258, 1983.

Rasmusson, E. M., Seasonal variation of tropical humidity parameters, in *General Circulation of the Tropical Atmosphere Vol. 1*, by R. E. Newell, J. W. Kidson, D. G. Vincent and G. J. Boer, pp. 193-237, MIT Press, Cambridge, Mass., 1972.

Read, W. G., J. W. Waters, D. A. Flower, L. Froidevaux, R. F. Jarnot, D. L. Hartmann, R. S. Harwood, and R. B. Rood, Upper-tropospheric water vapor from UARS MLS, *Bull. Am. Met. Soc., 76*, 2381-2389, 1995.

Reynolds, R. W. and T. M. Smith, A high-resolution global sea surface temperature climatology, *J. Clim., 8*, 1571-1583, 1995.

Rind, D., E.-W. Chiou, W. Chu, J. Larsen, S. Oltmans, J. Lerner, M. P. McCormick, and L. McMaster, Positive water vapour feedback in climate models confirmed by satellite data, *Nature, 349*, 500-503, 1991.

Soden, B. J. and R. Fu, A satellite analysis of deep convection, upper-tropospheric humidity, and the greenhouse effect, *J. Climate, 8*, 2333-2351, 1995.

Stephens, G. L., D. L. Jackson, and I. Whitmeyer, Global observations of upper-tropospheric water vapor derived from TOVS Radiance Data, *J. Climate, 9*, 305-326, 1996.

Wang, C., P. J. Crutzen, Y. Ramanathan and S. F. Williams, The role of a deep convective storm over the tropical Pacific Ocean in the redistribution of atmospheric chemical species, *J. Geophys. Res., 100*, 11509-11516, 1995.

Webster, P. J. and G. L. Stephens, Tropical upper-tropospheric extended clouds: Inferences from winter MONEX, *J. Atmos. Sci., 37*, 1521-1541, 1980.

Wu, Z.-X., The Influence of SST on Air Temperature in the Tropics, Ph.D. Thesis, 237 pp., MIT, Cambridge, Mass., March 1996.

Zimmerman, P. H., H. B. Selkirk, and R. E. Newell, The relationship between large-scale vertical motion, highly reflective cloud, and sea surface temperature in the tropical Pacific region, *J. Geophys. Res., 93*, 11205-11215, 1988.

R. E. Newell and Y. Zhu, Massachusetts Institute of Technology, 54-1824, 77 Massachusetts Ave., Cambridge, MA 02139. (e-mail: newell@NEWELL1.MIT.EDU; zhu@NEWELL1.MIT.EDU)

W. G. Read and J. W. Waters, Jet Propulsion Laboratory, California Institute of Technology, M/S 183-701, 4800 Oak Grove Dr., Pasadena, CA 91109-8099. (e-mail: bill@camel.jpl.nasa.gov; joe@jedediah.jpl.nasa.gov)

(Received June 19, 1996; revised November 13, 1996; accepted December 3, 1996.)